Electronic Supplementary Information: Charge and hydration structure of dendritic polyelectrolytes: molecular simulations of polyglycerol sulphate

Rohit Nikam,[1,2] Xiao Xu,[3] Matthias Ballauff,[4,2,5] Matej Kanduč,[1] and Joachim Dzubiella[1,6]

[1]*Research Group for Simulations of Energy Materials,*
Helmholtz-Zentrum Berlin für Materialien und Energie,
Hahn-Meitner-Platz 1, D-14109 Berlin, Germany
[2]*Institut für Physik, Humboldt-Universität zu Berlin,*
Newtonstr. 15, D-12489 Berlin, Germany
[3]*School of Chemical Engineering, Nanjing University of Science and Technology,*
200 Xiao Ling Wei, Nanjing 210094, P. R. China
[4]*Soft Matter and Functional Materials,*
Helmholtz-Zentrum Berlin für Materialien und Energie,
Hahn-Meitner-Platz 1, D-14109 Berlin, Germany
[5]*Multifunctional Biomaterials for Medicine, Helmholtz Virtual Institute,*
Kantstr. 55, D-14513 Teltow-Seehof, Germany
[6]*Physikalisches Institut, Albert-Ludwigs-Universität Freiburg,*
Hermann-Herder Str. 3, D-79104 Freiburg, Germany,

Email: joachim.dzubiella@helmholtz-berlin.de

I. FORCEFIELD PARAMETERS

The General Amber Force Field (GAFF)[1, 2] is employed to characterize atomistic interaction properties in all simulations. The bonded and nonbonded parameters for atoms in the system are displayed in the Tables S1–S4 below. The partial charges are summarized in Fig. S1.

Atomtype	σ (nm)	ϵ (kJ mol^{-1})	Description
C	0.340	0.458	sp3 carbon
CS	0.340	0.458	sp3 α-carbon to sulphate
OS	0.300	0.711	ether and ester oxygen
OB	0.300	0.711	sulphate oxygen connecting sulphate to dPG
O	0.296	0.878	sulphate oxygen
S	0.356	1.046	sulphate sulphur
H1	0.247	0.066	hydrogen connected to α-carbon to sulphate
HC	0.265	0.066	hydrogen connected to carbon
NA	0.333	0.011	Na^+ ion
CL	0.440	0.418	Cl^- ion

TABLE S1: Atom identities and corresponding nonbonded Lennard–Jones parameters used for dPGS molecules and ions in the simulation with the GAFF force field.

II. CALCULATION OF ATOMIC PARTIAL CHARGES

While the restrained electrostatic potential (RESP) method [3, 4] at the HF/6-31G* level is the default charge approach applied in the Amber protein force fields [1], this charge scheme requires to perform an ab initio optimization at the HF/6-31G* level, which prevents it from being used in handling large molecules such as dPGS. Alternatively, in this work, the partial charges of the dPGS atoms were calculated using the AM1-BCC quantum mechanical scheme [5], which is computationally much cheaper than HF/6-31G* RESP and is compatible with GAFF [1]. The Antechamber package [2, 6] from USCF Chimera software (Ver. 1.11.2) [7] is used to assign the partial charges.

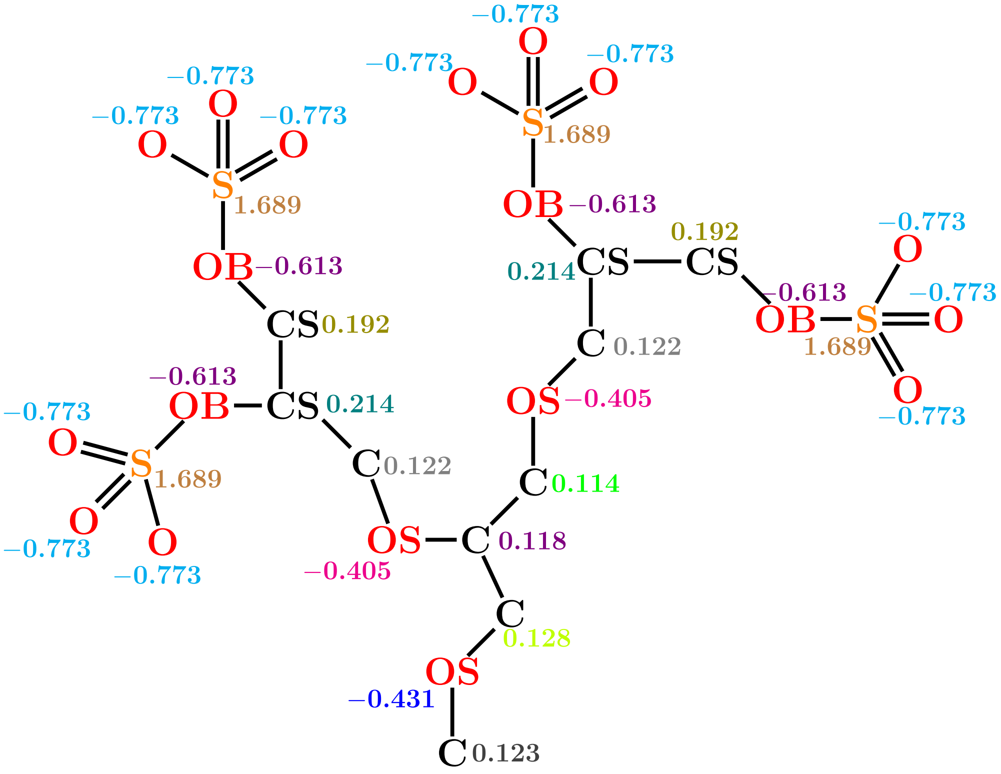

FIG. S1: The atomistic structure and the AM1–BCC partial charges (in units of e_0) for one of the three repeating main branches of G_1–dPGS [see Fig. 1(a) in the main text]. All accompanying hydrogens of carbons have a partial charge of 0.045 e_0.

Bonds	k_{ij}^b (kJ mol^{-1} nm^{-2})	b_{ij} (nm)
C–C	253634.0	0.154
C–CS	253634.0	0.154
CS–CS	253634.0	0.154
C–OS	252295.2	0.144
CS–OB	252295.2	0.144
OB–S	297064.0	0.157
S–O	452792.0	0.146
C–HC	282252.6	0.109
CS–H1	281081.1	0.109

TABLE S2: Bond parameters for the atoms in dPGS

Angles	k^{θ}_{ijk} (kJ mol^{-1})	θ^{0}_{ijk} (deg)
C–C–C	528.86	110.63
C–C–CS	528.86	110.63
C–CS–CS	528.86	110.63
C–C–OS	418.40	109.50
CS–C–OS	567.35	108.42
C–CS–OB	567.35	108.42
CS–CS–OB	567.35	108.42
C–OS–C	519.65	113.41
CS–OB–S	496.22	109.55
OB–S–O	624.25	107.84
O–S–O	624.25	119.82
H1–CS–OB	425.09	108.82
H1–CS–CS	388.27	110.07
H1–CS–C	388.27	110.07
H1–CS–H1	328.02	109.55
HC–C–HC	329.70	108.35
HC–C–C	388.27	110.05
HC–C–CS	388.27	110.05
HC–C–OS	425.93	108.70

TABLE S3: Angle parameters for the atoms in dPGS

Dihedrals	ϕ_s (deg)	k_ϕ (kJ mol^{-1})	Multiplicity (n)
C–C–C–OS	0.00	0.651	3
CS–CS–C–OS	0.00	0.651	3
C–CS–CS–OB	0.00	0.651	3
OS–C–C–OS	0.00	0.651	3
OS–C–CS–OB	0.00	0.651	3
OB–CS–CS–OB	0.00	0.651	3
C–OS–C–C	180.0	0.418	2
C–OS–C–CS	180.0	0.418	2
C–CS–OB–S	0.00	1.604	3
CS–CS–OB–S	0.00	1.604	3
CS–OB–S–O	180.0	5.020	2
HC–C–C–HC	0.00	0.620	3
HC–C–CS–H1	0.00	0.620	3
H1–CS–CS–H1	0.00	0.620	3
HC–C–C–C	0.00	0.670	3
H1–CS–CS–C	0.00	0.670	3
HC–C–CS–CS	0.00	0.670	3
HC–C–OS–C	0.00	1.604	3
H1–CS–OB–S	0.00	1.604	3
HC–C–C–OS	0.00	1.046	1
H1–CS–C–OS	0.00	1.046	1
H1–CS–CS–OS	0.00	1.046	1
HC–C–CS–OS	0.00	1.046	1
HC–C–CS–OB	0.00	1.046	1
H1–CS–CS–OB	0.00	1.046	1

TABLE S4: Dihedral parameters for the atoms in dPGS

III. SOLVENT ACCESSIBLE SURFACE AREA AND VOLUME

The solvent accessible surface area (SASA) and solvent excluded volume characterize the interaction of dendrimer with the solvent. Although the outer surface of dPGS exposed to water is available for interaction, there still remains a significant accessible internal surface area in the dendrimer. To evaluate the solvent accessible surface area and volume, each atom is assumed as a sphere with the radius r_i that is the sum of the van der Waals radius of that atom r_{vdW} and a probe radius r_p, *i.e.*, $r_i = r_{vdW} + r_p$. The dendrimer is assumed as the union of fused spheres. The SASA is defined as the surface traced by the spherical solvent probe as it rolls around the van der Waals spheres of the dendrimer. Fig. S2(a) plots $\sqrt{\text{SASA}}$ as a function of the probe radius. We can see that at a constant probe radius, it increases with increasing number of generations and also increases linearly with the probe radius (except for small values of the probe radius)[8]. For each dPGS generation, as the probe radius gets smaller, we see deviations from the linear behaviour due to the extra surface in the interior of the dendrimer. Assuming the shape of the dendrimer to be spherical, we can estimate the exterior surface area and the size of the dendrimer from these plots using linear regression. For such a case SASA is given by $\text{SASA} = 4\pi(R_{\text{SA}} + r_p)^2$. The radius of the dendrimer R_{SA} is thus calculated for the probe radius of 0.14 nm, which is the radius of the water molecule. The values of R_{SA} are given in Table S5. The difference between the calculated points and the regression line gives the internal area Σ of the pores and voids. The values of Σ for different generations are listed in Table S5 for a probe radius of 0.14 nm. We can observe that the available internal surface area increases sharply with generation.

The volume associated with these internal cavities can also be estimated by calculating the solvent accessible volume, V_{SA}. For a perfect sphere without any cavities it is given by $V_{\text{SA}} = \frac{4}{3}\pi(R_{\text{VSA}} + r_p)^3$. Fig. S2(b) shows $\sqrt[3]{V_{\text{SA}}}$ as a function of the probe radius for different generations. We see that it scales linearly with the probe radius for its higher values. The estimates of the size R_{VSA} of the dendrimer for a probe radius of 0.14 nm are listed in Table S5. The deviation of V_{SA} from the regression line in Fig. S2(b) gives an estimate for the volume Λ of the pores and voids in the dendrimer. The values of Λ for different generations are listed in Table S5 for a probe radius of 0.14 nm.

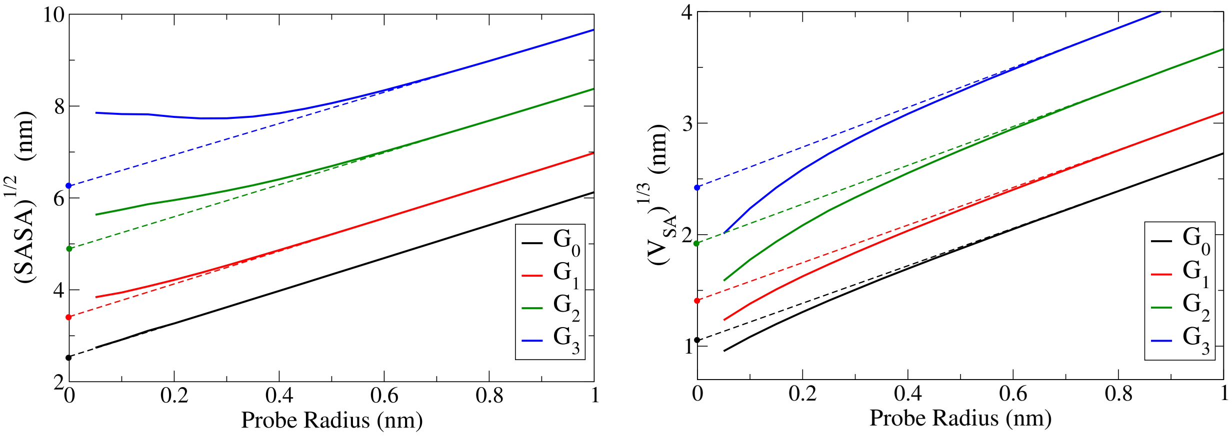

FIG. S2: (a) $\sqrt{\mathrm{SASA}}$ and (b) $\sqrt[3]{V_{\mathrm{SA}}}$ as a function of the probe radius.

	G_0	G_1	G_2	G_3
SASA [nm^2]	9.56	16.60	34.38	61.16
R_{SA} [nm]	0.72	0.96	1.38	1.76
V_{SA} [nm^3]	1.15	2.76	7.06	14.14
R_{VSA} [nm]	0.65	0.87	1.19	1.50
Σ [nm^2]	0.00	0.20	2.50	14.00
Λ [nm^3]	0.00	0.02	0.07	0.09

TABLE S5: Results of SASA and V_{SA} calculations, for a probe radius of 0.14 nm (radius of the water molecule). R_{SA} and R_{VSA} stand for the radius of dPGS estimated via calculation of SASA and of V_{SA}, respectively. Σ and Λ define the surface area and the volume of the voids inside dPGS, respectively.

IV. EXPLICIT VS. IMPLICIT WATER INTEGRATION: CUMULATIVE CHARGE AND ELECTROSTATIC FIELDS

Figs. S3 and S4 show the comparison of explicit and implicit water approaches in terms of the ratio of the net cumulative charge and the dielectric constant $Z(r)/\epsilon_{\mathrm{r}}$ and the resultant electrostatic field $e_0E(r)$ as a function of the distance from the dPGS-COM, for all generations. Evidently, $E(r)$ from explicit water profiles exhibits spacially correlated noise, which stems from the integration of the noise in the charge density of water. This latter charge density is obtained by summing the individual charge densities of hydrogen and oxygen atoms of water.

We now take an illustrative example of an electroneutral system, where we have $\langle N\rangle$ positive and $\langle N\rangle$ negative charges in a sampling bin. The difference between the positive and negative charges is zero on average. However, their statistical uncertainty (noise) scales as $\sim\sqrt{\langle N\rangle}$, which indicates that the higher the charge density, the higher the uncertainty of the difference. This effect can normally be observed in large bins (*i.e.*, for large r) contain-

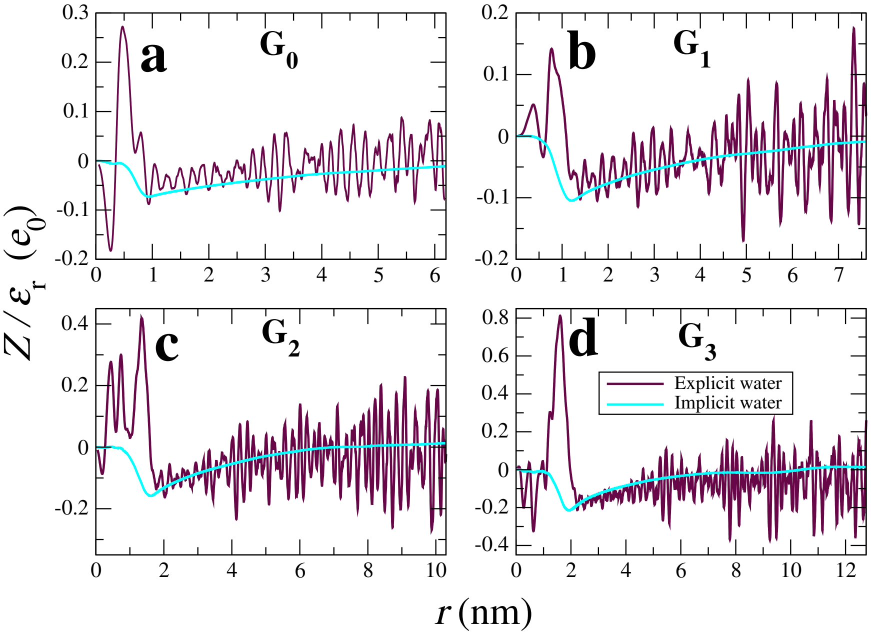

FIG. S3: Comparison of the ratio of the net cumulative charge distribution and the dielectric constant with respect to dPGS-COM between the implicit and explicit water integration approaches. For the implicit water approach $\epsilon_{\mathrm{r}} = 72$, while for the explicit approach, $\epsilon_{\mathrm{r}} = 1$.

ing large number of water molecules. Since dPGS is a highly charged molecule, we used significantly large sizes of the simulation box (listed in Table 1 of the main text) in order to ensure that the bulk regime is reached in far-field. However, the downside of this strategy is an increase in the statistical uncertainty in the charge calculations of water in the explicit water approach. This effect can be reduced by a sufficient time averaging, thus performing longer simulations.

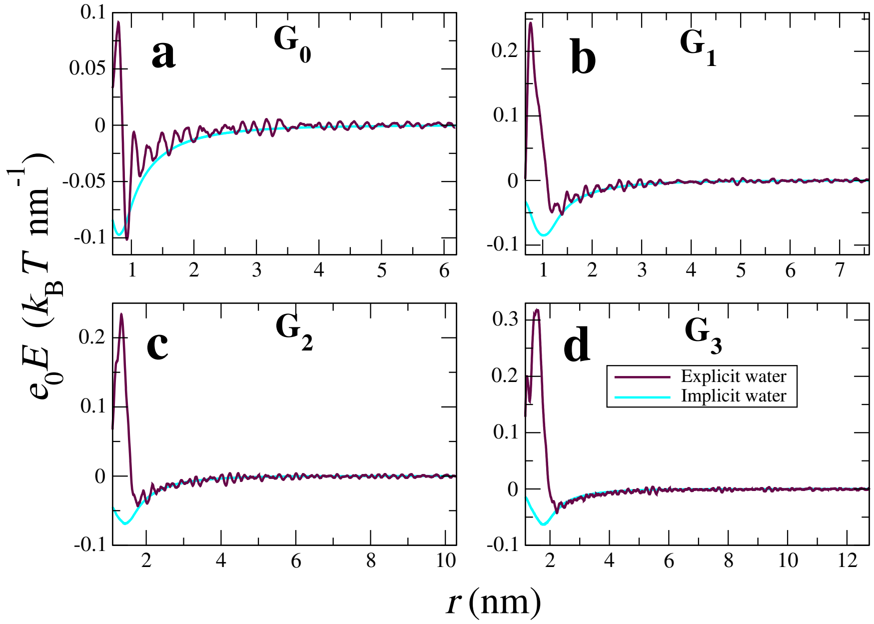

FIG. S4: Comparison of electrostatic field profiles with respect to dPGS-COM between the implicit and explicit water integration approaches.

Bibliography

[1] J. Wang, R. M. Wolf, J. W. Caldwell, P. A. Kollman, and D. A. Case, J. Comput. Chem. **25**, 1157 (2004).

[2] J. Wang, W. Wang, P. A. Kollman, and D. A. Case, J. Mol. Graphics Modell. **25**, 247 (2006).

[3] C. I. Bayly, P. Cieplak, W. Cornell, and P. A. Kollman, J. Phys. Chem. **97**, 10269 (1993).

[4] P. Cieplak, W. D. Cornell, C. Bayly, and P. A. Kollman, J. of Comput. Chem. **16**, 1357 (1995).

[5] A. Jakalian, D. B. Jack, and C. I. Bayly, J. Comput. Chem. **23**, 1623 (2002).

[6] J. Wang, W. Wang, P. A. Kollman, and D. A. Case, J. Am. Chem. Soc. **222**, U403 (2001).

[7] E. F. Pettersen, T. D. Goddard, C. C. Huang, G. S. Couch, D. M. Greenblatt, E. C. Meng, and T. E. Ferrin, J. Comput. Chem. **25**, 1605 (2004).

[8] P. K. Maiti, T. Çagin, S.-T. Lin, and W. A. Goddard, Macromolecules **38**, 979 (2005).